Proceedings of the 34th Chinese Control Conference
July 28-30, 2015, Hangzhou, China

Model-Based Line-of-Sight Detection of an Irregular Celestial Body for Autonomous Optical Navigation

WU Qian[1], ZOU Wei[1], XU De[1], MAO Xiaoyan[2]

1. Institute of Automation, Chinese Academy of Sciences, Beijing 100190
E-mail: qian.wu@ia.ac.cn

2. Beijing Institute of Control Engineering, Beijing 100094

Abstract: This paper proposes a model-based line-of-sight (LOS) determination system with high-precision for irregular celestial bodies applied in autonomous optical navigation. The 3D model of the target celestial body is assumed to be given in the task. The proposed system utilizes the 3D model to construct a 2D figure feature database. These 2D figures are extracted from regular sampled viewpoints in a sphere surface, and the selected features represent the contour shape of the figures and the corresponding LOS information. Then, a LOS determination system is developed based on the 2D figure feature database. The system detects the LOS unit vector of a given image though three steps. Firstly, the contour features of the target celestial body are extracted from the given image. Secondly, the best matching template is searched out from the database based on shape similarity of the contour. Thirdly, the LOS unit vector of the given image is generated by using the LOS information of the searched template based on similarity principle. Experiment results demonstrate the effectiveness and advantages of the proposed method.

Key Words: autonomous optical navigation, line-of-sight detection, image processing, centroid extraction, irregular celestial body

1 Introduction

Nowadays, autonomous optical navigation becomes a research hotspot in deep space navigation for its less time consumption, higher precision, and higher efficiency compared with traditional navigation methods, such as ground based navigation[1]. In optical navigation tasks, onboard cameras carried by a spacecraft are adopted to capture the images of the target celestial body. Then, these images are processed to extract various parameters, including the line-of-sight (LOS) vector, apparent diameter, etc[2]. Among these, the LOS vector which comes from the optical center of the camera to the centroid of the target celestial body (CTCB) is a vital parameter to determine the spacecraft's position and attitude[3]. According to the camera model, the LOS direction is determined by the image coordinate of the CTCB. Therefore, detection the imaging point of CTCB becomes critically important for autonomous optical navigation.

With the development of deep space missions, there are many reports published on the subject of LOS detection for autonomous optical navigation. The existing LOS detection techniques can be classified into three categories. In the first category, the brightness center (BC) of the target body image is adopted as the imaging point of CTCB to determine the LOS direction. Mastrodemos et al.[4] proposed an autonomous optical navigation system for the deep impact mission encounter with comet Tempel 1, and a BC extraction algorithm was developed in this paper. In the second category, the figure center (FC) of the target body is adopted as the imaging point of CTCB. Bhaskaranet al.[5] proposed an autonomous nucleus tracking system for comet/asteroid encounters, using STARDUST mission as an example. In the system, the FC was determined by refining the BC with an offset. In the third category, the target celestial body is assumed to be a sphere approximately. Therefore, the image figure of the target body is an ellipse, and the center of the ellipse is used as the imaging point of CTCB. Christian et al.[6] proposed an onboard image processing algorithm for a spacecraft optical navigation sensor system. The main objective of the algorithm was to extract the ellipse center in the captured image. Li et al.[7] proposed an improved ellipse extracting algorithm for LOS detection. Wu et al.[8] analyzed the FC method and the ellipse extracting method, and made comparisons between the two methods.

All the above researches are suitable for symmetrical or spherical target bodies. However, when applied to an irregular target body, high precision solution can hardly be achieved. This paper proposed a model-based LOS determination system with high precision for an irregular target celestial body. In deep space mission, the spacecraft usually stays in observation orbit for at least half a year to obtain certain features of the target celestial body, such as size, mass, gravity field, 3D surface topography and so on[9]. Therefore, the 3D model of the target celestial body can be assumed to be given in this task. Since the imaging figure of an irregular body varies with the change of view angle, a 2D figure feature database is constructed to reserve the shape features of the figures and the corresponding imaging point of CTCB from a group of regular sampled viewpoints based on the 3D model. Then, the LOS determination system is developed based on the 2D figure feature database. The feasibility and advantages of the proposed method are verified by several representative experiments.

2 Problem Statement and Overall Solution

2.1 Problem Statement

The objective of this paper is to detect the LOS direction of an irregular target celestial body using the image captured

by onboard optical devices i.e. cameras. The LOS vector comes from the optical center of the onboard camera to CTCB, as Fig.1 shown. Denote $O_CX_CY_CZ_C$ and $O_TX_TY_TZ_T$ as the coordinate systems of the camera and the target body respectively. O_C is the optical center of the camera, and O_T is CTCB. Obviously, vector $\overrightarrow{O_CO_T}$ is the LOS vector. Denote $({}^C x_T, {}^C y_T, {}^C z_T)$ as the coordinate of O_T in the camera coordinate system. We use the unit vector $\mathbf{L_U}$ to represent the LOS direction, and L_U can be calculated as

$$\mathbf{L_U} = \frac{\overrightarrow{O_CO_T}}{\left\|\overrightarrow{O_CO_T}\right\|} = \frac{\begin{bmatrix} {}^C x_T & {}^C y_T & {}^C z_T \end{bmatrix}^T}{\sqrt{{}^C x_T{}^2 + {}^C y_T{}^2 + {}^C z_T{}^2}} \tag{1}$$

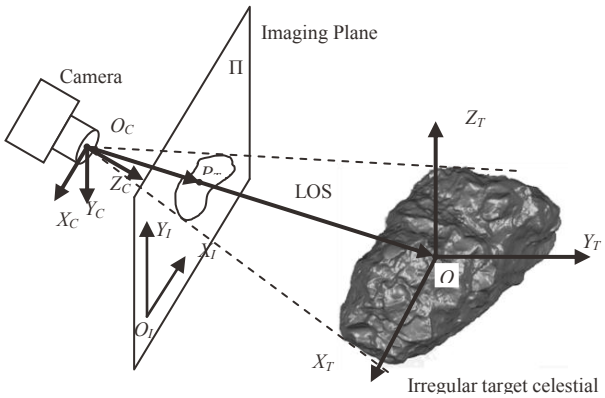

Fig. 1: The geometry of LOS direction

Plane Π is the imaging plane of the camera, and P_T is the imaging point of O_T. Denote $O_IX_IY_I$ as the coordinate system of the image. Denote $({}^I x_T, {}^I y_T)$ as the image coordinate of P_T, and. According to the pinhole camera model[10], we have

$$s\begin{bmatrix} {}^I x_T \\ {}^I y_T \\ 1 \end{bmatrix} = \mathbf{A}\begin{bmatrix} {}^C x_T \\ {}^C y_T \\ {}^C z_T \end{bmatrix} = \begin{bmatrix} k_x & 0 & {}^I x_0 \\ 0 & k_y & {}^I y_0 \\ 0 & 0 & 1 \end{bmatrix}\begin{bmatrix} {}^C x_T \\ {}^C y_T \\ {}^C z_T \end{bmatrix} \tag{2}$$

where $\mathbf{A}$ is the camera intrinsic matrix, $({}^I x_0, {}^I y_0)$ is the coordinate of the principal point in image coordinate system, and k_x and k_y are the scale factors in image X and Y axes respectively. Therefore, $({}^C x_T, {}^C y_T, {}^C z_T)$ is given as

$$\left({}^C x_T, {}^C y_T, {}^C z_T\right) = \left(\frac{({}^I x_T - {}^I x_0)}{k_x}{}^C z_T, \frac{({}^I y_T - {}^I y_0)}{k_y}{}^C z_T, {}^C z_T\right) \tag{3}$$

Substituting formula (3) into formula (1), $\mathbf{L_U}$ is given as

$$\mathbf{L_U} = \frac{\begin{bmatrix} k_y({}^I x_T - {}^I x_0) & k_x({}^I y_T - {}^I y_0) & k_x k_y \end{bmatrix}^T}{\sqrt{\left(k_y{}^2({}^I x_T - {}^I x_0)^2 + k_x{}^2({}^I y_T - {}^I y_0)^2 + k_x{}^2 k_y{}^2\right)}} \tag{4}$$

In formula (4), k_x and k_y are constant when the optical settings of the onboard camera keep unchanged. The value of k_x and k_y can determined by camera calibration easily. Thus, the LOS unit vector is determined by the image coordinate of CTCB.

2.2 Overall Solution

According to the above conclusions, the objective of the proposed system is to extract the imaging point of CTCB. For an irregular target, the imaging point of CTCB and the imaging shape of the target body varies when the camera's view angle changes. Moreover, the view angle of two images changes smaller, the shift of the imaging point of CTCB in the images is smaller, and the imaging shape of the target body changes smaller. Therefore, based on the 3D model of the target celestial body, the proposed method constructs a 2D figure feature database, which reserves the figure features and the corresponding imaging point of CTCB. And the 2D figures are extracted from regular sampled view angle. Accordingly, the imaging point of CTCB in a captured image of the target body can be determined by the information of the similar 2D figure searched in the database. Based on the above strategy, the proposed system consists of two stages: 1. 2D figure feature database construction, 2. imaging point of CTCB determination, as Fig.2 shown.

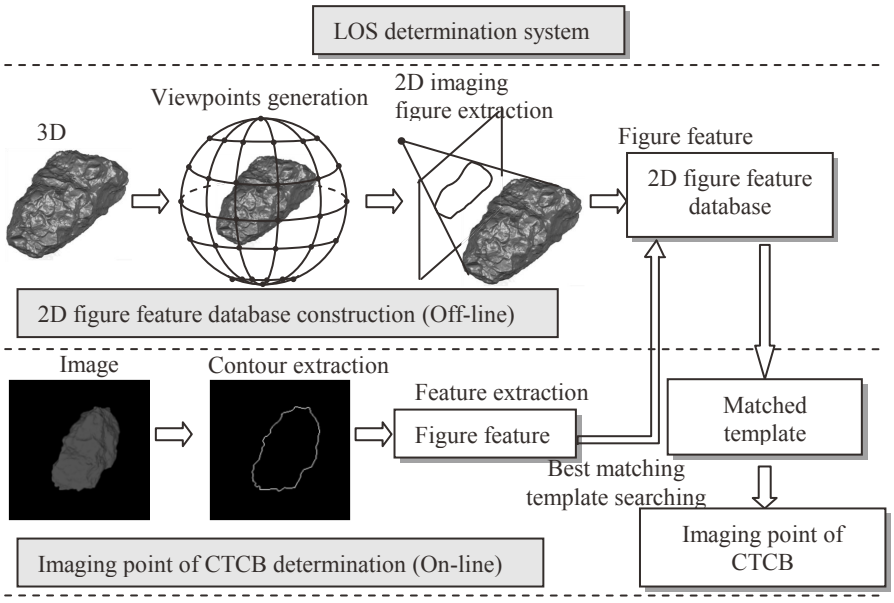

Fig. 2: Overall procedure of the proposed method

3 2D figure feature database construction

3.1 Viewpoint Generation

As mentioned in above section, the viewpoints are generated at a regular angle interval. Moreover, the distance between the target celestial body and the onboard camera has little influence to the imaging shape of the target celestial body, when the distance is much larger than the long axis of the target celestial body and the view angle keeps invariant. Therefore, the viewpoints are sampled on a viewing sphere at regular angle interval, as Fig. 3 shown. The centre of the viewing sphere is located at CTCB. The radius is set about 3 times of the long axis of the target celestial body. Denote α and β as the latitude and longitude of a sampled viewpoint respectively, and denote R as the radius of the viewing sphere. Then, the coordinate of a sampled viewpoint in the target body coordinate system is given as

$$\left({}^{T}x_v, {}^{T}y_v, {}^{T}z_v\right) = \left(R\sin\alpha\cos\beta, R\sin\alpha\sin\beta, R\cos\alpha\right) \quad (5)$$

where

$$\begin{cases} \alpha = n_1\Delta, n_1 = 0,\cdots,\left[\dfrac{180}{\Delta}\right] \\ \beta = n_2\Delta, n_2 = 0,\cdots,\left[\dfrac{360}{\Delta}\right]\text{-}1 \end{cases}$$

where Δ is the sampling angle interval. Then, the viewpoint set VP is given as

$$VP = \left\{ vp_i : \left({}^{T}x_{vp}, {}^{T}y_{vp}, {}^{T}z_{vp}\right)_i \middle| i = 1,\cdots,N_{VP} \right\}$$

where

$$N_{VP} = \left(\left[\frac{180}{\Delta}\right] - 2\right)\cdot\left[\frac{360}{\Delta}\right] + 2 \quad (6)$$

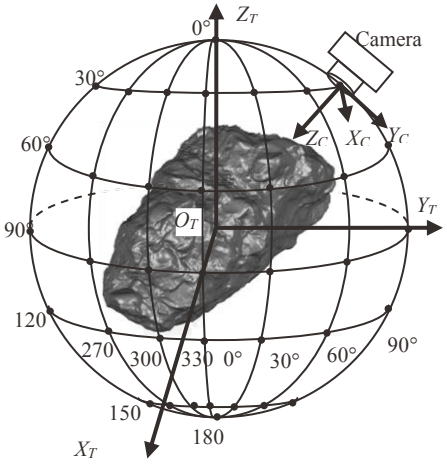

Fig. 3: Viewpoint sampling

The camera will locate at the sampled viewpoints to extract the imaging figure of the target celestial body, and the optical axis of the camera is point to the origin of the target body coordinate system as well as CTCB. Then, a camera coordinate system is established there accordingly. For the approach in next section, the transform matrix from the camera coordinate system to the target body coordinate system is generated as

$${}^{\mathbf{T}}\mathbf{T}_{\mathbf{C}} = \begin{bmatrix} \cos\alpha\cos\beta & \sin\beta & -\sin\alpha\cos\beta & R\sin\alpha\cos\beta \\ \cos\alpha\sin\beta & -\cos\beta & -\sin\alpha\sin\beta & R\sin\alpha\sin\beta \\ -\sin\alpha & 0 & -\cos\alpha & R\cos\alpha \\ 0 & 0 & 0 & 1 \end{bmatrix} \quad (7)$$

3.2 2D Imaging Figure Extraction

After viewpoint sampling, the 2D imaging figures of the target celestial body are extracted from these viewpoints based on the 3D model. In this paper, the 3D model is in Stereolithography (STL) format, since it is widely used as an industry standard with advantages of simplicity and robustness[11]. The STL file represents a triangular mesh model, consisting of vertexes and normal vectors in a group of facets[12]. In this task, only the vertex and edge information are concerned. After loading the STL file, the triangular meshes is represented as

$$V : \left\{ v_i : \left({}^{T}x_v, {}^{T}y_v, {}^{T}z_v\right)_i \middle| i = 1,\cdots,N_V \right\}$$

$$E : \left\{ e_j : \left(IV_{first}, IV_{second}\right)_j \middle| j = 1,\cdots,N_E \right\}$$

where V and E represent the vertex sequence and the edge sequence respectively, IV represents the index of the vertexes.

Since the contour shape of the imaging figure is the critical characteristic for best matching template searching. The 2D figure is represented by a contour chain, which consists of a link of points around the shape of the figure

$$CC : \left\{ cc_i : \left({}^{I}x_{cc}, {}^{I}y_{cc}\right)_i, i = 1,\cdots,N_{CC} \right\}$$

where cc_i is a point in the contour. The procedure for the contour chain generation is summarized as followed.

1. Calculate the imaging points of all vertexes in the triangular meshes;
2. Link the two imaging points in one edge of a facet;
3. Detect the contour chain by Moore-Neighbor Contour Tracing Algorithm.

Firstly, the pinhole camera model is adopted to calculate the imaging points of all vertexes in the triangular meshes from a sampled viewpoint. Assume ip_i is the imging point of the vertex v_i. Denote $({}^{I}x_i, {}^{I}y_i)$ as the coordinate of ip_i in the image coordinate system, and denote $({}^{T}x_i, {}^{T}y_i, {}^{T}z_i)$ and $({}^{C}x_i, {}^{C}y_i, {}^{C}z_i)$ as the coordinate of v_i in the target body and camera coordinate system respectively. According to the pinhole camera model, the followed equations can be obtained

$$\begin{cases} s\begin{bmatrix} {}^{I}x_i \\ {}^{I}y_i \\ 1 \end{bmatrix} = \mathbf{A}\begin{bmatrix} {}^{C}x_i \\ {}^{C}y_i \\ {}^{C}z_i \end{bmatrix} = \begin{bmatrix} k_x & 0 & {}^{I}x_0 \\ 0 & k_y & {}^{I}y_0 \\ 0 & 0 & 1 \end{bmatrix}\begin{bmatrix} {}^{C}x_i \\ {}^{C}y_i \\ {}^{C}z_i \end{bmatrix} \\ \begin{bmatrix} {}^{C}x_i \\ {}^{C}y_i \\ {}^{C}z_i \\ 1 \end{bmatrix} = {}^{\mathbf{T}}\mathbf{T}_{\mathbf{C}}^{-1}\begin{bmatrix} {}^{T}x_i \\ {}^{T}y_i \\ {}^{T}z_i \\ 1 \end{bmatrix} = {}^{\mathbf{C}}\mathbf{T}_{\mathbf{T}}\begin{bmatrix} {}^{T}x_i \\ {}^{T}y_i \\ {}^{T}z_i \\ 1 \end{bmatrix} = \begin{bmatrix} {}^{\mathbf{C}}\mathbf{L}_{\mathbf{T1}}{}^{T} \\ {}^{\mathbf{C}}\mathbf{L}_{\mathbf{T2}}{}^{T} \\ {}^{\mathbf{C}}\mathbf{L}_{\mathbf{T3}}{}^{T} \\ {}^{\mathbf{C}}\mathbf{L}_{\mathbf{T4}}{}^{T} \end{bmatrix}{}^{\mathbf{T}}\mathbf{X}_{\mathbf{i}} \end{cases} \quad (8)$$

where ${}^{\mathbf{C}}\mathbf{T}_{\mathbf{T}}$ is the inverse matrix of ${}^{\mathbf{T}}\mathbf{T}_{\mathbf{C}}$, which is given by formula (7) and means the transform matrix from the camera coordinate system to the target body coordinate system. ${}^{\mathbf{C}}\mathbf{L}_{\mathbf{T1}}{}^{T}$, ${}^{\mathbf{C}}\mathbf{L}_{\mathbf{T2}}{}^{T}$, ${}^{\mathbf{C}}\mathbf{L}_{\mathbf{T3}}{}^{T}$, and ${}^{\mathbf{C}}\mathbf{L}_{\mathbf{T4}}{}^{T}$ are the row vectors of ${}^{\mathbf{C}}\mathbf{T}_{\mathbf{T}}$, and ${}^{\mathbf{T}}\mathbf{X}_{\mathbf{i}}$ is the vector $[{}^{T}x_i\ {}^{T}y_i\ {}^{T}z_i\ 1]^{\mathrm{T}}$. Then, the coordinate of ip_i is derived as

$$\begin{cases} {}^{I}x_i = k_x \dfrac{{}^{C}\mathbf{L}_{T1}{}^{T}\,{}^{T}\mathbf{X}_i}{{}^{C}\mathbf{L}_{T3}{}^{T}\,{}^{T}\mathbf{X}_i} + {}^{I}x_0 \\ {}^{I}y_i = k_y \dfrac{{}^{C}\mathbf{L}_{T2}{}^{T}\,{}^{T}\mathbf{X}_i}{{}^{C}\mathbf{L}_{T3}{}^{T}\,{}^{T}\mathbf{X}_i} + {}^{I}y_0 \end{cases} \tag{9}$$

Secondly, the two imaging points in the same edge are linked according to the edge sequence *E*. Therefore, the imaging information of the vertexes and edges in the 3D model are recorded in the binary image, as Fig. 4 shown. The black squares represent the projection of the vertexes, and the gray squares represent the projection of the edges.

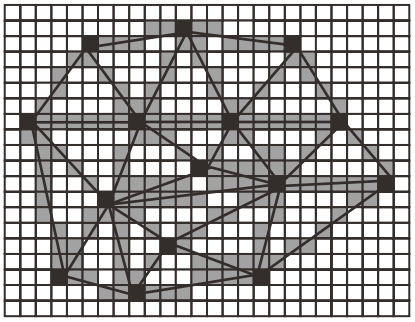

Fig. 4: The binary image of the 2D figure

Thirdly, Moore-Neighbor Contour Tracing algorithm[13] (MNCTA) is adopted to detect the contour chain in the binary image.

3.3 Figure Feature Selection

After the figure extraction, several features are chosen to represent some characteristics of these figures. Firstly, the database should reserve the coordinate of the imaging point of CTCB. Secondly, since the shape similarity between figures is the basis for template matching, Hu moments are adopted to represent the shape characteristics of these figures. Particularly, Hu moments are invariant to the translation, rotation, and scaling of objects[14]. Thus, some parameters are adopted to represent the position, attitude, and size information of these figures. The position of the figure is represented by the center point of the figure. The size of the figure is represented by the area of the figure. The attitude of the figure is represented by the attitude vector, which come from the center point to the furthest point in the contour chain.

Since the optical axis of the camera points to CTCB, the imaging point of CTCB is the principal point $({}^{I}x_0, {}^{I}y_0)$.

Hu moments consist of seven invariant moments.

$$\mathbf{H}=\begin{bmatrix} h_1 & h_2 & h_3 & h_4 & h_5 & h_6 & h_7 \end{bmatrix}^T \tag{10}$$

where

$$\begin{cases} h_1 = \eta_{20} + \eta_{02} \\ h_2 = (\eta_{20} - \eta_{02})^2 + 4\eta_{11}{}^2 \\ h_3 = (\eta_{30} - 3\eta_{12})^2 + (3\eta_{21} - \eta_{03})^2 \\ h_4 = (\eta_{30} + \eta_{12})^2 + (\eta_{21} + \eta_{03})^2 \\ h_5 = (\eta_{30} - 3\eta_{12})(\eta_{30} + \eta_{12})\left[(\eta_{30} + \eta_{12})^2 - 3(\eta_{21} + \eta_{03})^2\right] \\ \quad +(3\eta_{21} - \eta_{03})(\eta_{21} + \eta_{03})\left[3(\eta_{30} + \eta_{12})^2 - (\eta_{21} + \eta_{03})^2\right] \\ h_6 = (\eta_{20} - \eta_{02})\left[(\eta_{30} + \eta_{12})^2 - (\eta_{21} + \eta_{03})^2\right] \\ \quad +4\eta_{11}(\eta_{30} + \eta_{12})(\eta_{21} + \eta_{03}) \\ h_7 = (3\eta_{21} - \eta_{03})(\eta_{30} + \eta_{12})\left[(\eta_{30} + \eta_{12})^2 - 3(\eta_{21} + \eta_{03})^2\right] \\ \quad -(\eta_{30} - 3\eta_{12})(\eta_{21} + \eta_{03})\left[3(\eta_{30} + \eta_{12})^2 - (\eta_{21} + \eta_{03})^2\right] \end{cases} \tag{11}$$

where

$$\eta_{pq} = \frac{\iint_D (x-\bar{x})^p (y-\bar{y})^q f(x,y)\,dxdy}{\left(\iint_D f(x,y)\,dxdy\right)^{(p+q+2)/2}} \tag{12}$$

In this paper, only the shape of the figure is concerned. Therefore, the gray value of pixels inside the contour are supposed to be 1, and the gray value of pixels outside the contour are supposed to be 0. Then, formula (12) is updated as

$$\eta_{pq} = \frac{\iint_{D_F} (x-\bar{x})^p (y-\bar{y})^q\,dxdy}{\left(\iint_{D_F} dxdy\right)^{(p+q+2)/2}} \tag{13}$$

where D_F is the figure area of the target body. A fast moment generation algorithm based on a contour chain proposed by Liu[15] is adopted.

Denote $(\bar{x}, \bar{y})$ as the center point of the figure, *S* as the area of the figure, and vector $\overrightarrow{CF}$ as the attitude vector. The position of the figure is represented by. The size of the figure is represented by *S*, which is given as

$$S = u_{00} = -\frac{1}{2}\sum_{i=1}^{N}(y_i x_{i-1} - x_i y_{i-1}) \tag{14}$$

The attitude of the figure is represented by $\overrightarrow{CF}$, which come from the center point *C* to the furthest point in the contour chain.

4 Imaging point of CTCB Determination

In the previous approaches, the 2D figure feature database has been constructed based on the 3D model of the target celestial body. Then, the imaging point of CTCB of a given image will be determined by the LOS determination system based on the database. The whole procedure includes contour feature extraction, best matching template searching, and imaging point of CTCB calculation.

Firstly, the figure contour of the target celestial body is extracted from the given image though image distortion correction, image smoothing, threshold segmentation, and edge detection. Using MNCTA presented in Sec. 3.2, the contour chain of this figure is detected. Then, the features of the given image, including Hu moments H_G, center point $(\bar{x}_G, \bar{y}_G)$, area S_G, and attitude vector (x_{GCF}, y_{GCF}), are generated according to the approaches presented in Sec. 3.2.

Secondly, the best matching template of the given image is searched from the database based shape similarity. The shape similarity error between figure F_i and figure F_j is defined as

$$SE\left(F_i,F_j\right)=\sum_{l=1}^{7}\lambda_l\left|h_l^i-h_l^j\right| \tag{15}$$

where $\left[h_1^i \quad h_2^i \quad h_3^i \quad h_4^i \quad h_5^i \quad h_6^i \quad h_7^i\right]^T$ and $\left[h_1^j \quad h_2^j \quad h_3^j \quad h_4^j \quad h_5^j \quad h_6^j \quad h_7^j\right]^T$ are the Hu moments of F_i and F_j respectively. In this system, the weight λ_n is defined as

$$\lambda_l=\max\left\{\left|h_l^m-h_l^n\right|\middle|F_m,F_n\in DF\right\} \tag{16}$$

where DF is the group of the figure templates in the database. The best matching template F_B of the given figure F_G is determined by

$$SE\left(F_B,F_G\right)=\min\left\{SE(F_i,F_G)\middle|F_i\in DF\right\} \tag{17}$$

Thirdly, the best matching template is utilized to calculate the imaging point of CTCB in the given image. Apparently, the searched template has the similar shape to the given figure, as Fig.5 shown. Therefore, through translation, rotation, and scaling transformation, the two figures become overlapping.

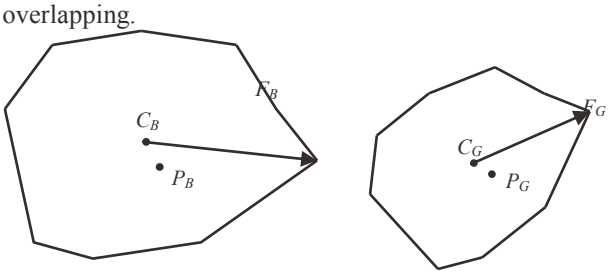

(a) The template figure (b) The given figure

Fig. 5 The shape of the template figure and the given figure

Denote C_B and C_G as the center point of the template figure and the given figure respectively. Denote P_B and P_G as the imaging point of CTCB in the template and the given figure respectively. Denote $\overrightarrow{C_BF_B}$ and $\overrightarrow{C_GF_G}$ as the attitude vector in the template and the given figure respectively. According to the similarity principle between two figures, the followed equations can be derived

$$\overrightarrow{C_GF_G}=k_cRot\left(\theta\right)\overrightarrow{C_BF_B} \tag{18}$$

$$\overrightarrow{C_GP_G}=k_cRot\left(\theta\right)\overrightarrow{C_BP_B} \tag{19}$$

where

$$k_c=\sqrt{\frac{S_G}{S_B}} \tag{20}$$

$$Rot\left(\theta\right)=\begin{bmatrix}\cos\theta & -\sin\theta\\ \sin\theta & \cos\theta\end{bmatrix} \tag{21}$$

k_c is the scale value, θ is the rotation angle, and S_B is the area of the template figure.

Apparently, vector $\overrightarrow{C_BF_B}$, the value of S_B, and the coordinates of C_B and P_B can be obtained from the database. Substituting them into formula (18) yields

$$\begin{bmatrix}\sin\theta\\ \cos\theta\end{bmatrix}=\begin{bmatrix}\sqrt{\frac{S_B}{S_G}}\left(\frac{x_{BCF}y_{GCF}-y_{BCF}x_{GCF}}{x_{BCF}^2+y_{BCF}^2}\right)\\ \sqrt{\frac{S_B}{S_G}}\left(\frac{x_{BCF}x_{GCF}+y_{BCF}y_{GCF}}{x_{BCF}^2+y_{BCF}^2}\right)\end{bmatrix} \tag{22}$$

where (x_{GCF},y_{GCF}) is the vector $\overrightarrow{C_GF_G}$, (x_{BCF},y_{BCF}) is the vector $\overrightarrow{C_BF_B}$. Then, the rotation angle θ is given as

$$\theta=\operatorname{atan2}\left(\sqrt{\frac{S_B}{S_G}}\left(\frac{x_{BCF}y_{GCF}-y_{BCF}x_{GCF}}{x_{BCF}^2+y_{BCF}^2}\right),\sqrt{\frac{S_B}{S_G}}\left(\frac{x_{BCF}x_{GCF}+y_{BCF}y_{GCF}}{x_{BCF}^2+y_{BCF}^2}\right)\right) \tag{23}$$

Substituting formula (23) into formula (19) yields

$$\begin{bmatrix}x_{GP}-x_{GC}\\ y_{GP}-y_{GC}\end{bmatrix}=\sqrt{\frac{S_G}{S_B}}\begin{bmatrix}\cos\theta & -\sin\theta\\ \sin\theta & \cos\theta\end{bmatrix}\begin{bmatrix}x_{BP}-x_{BC}\\ y_{BP}-y_{BC}\end{bmatrix} \tag{24}$$

where (x_{GP},y_{GP}), (x_{GC},y_{GC}), (x_{BP},y_{BP}), (x_{BP},y_{BP}) are the coordinate of P_G, C_G, P_B and C_B respectively. Therefore, the coordinate of the imaging point of CTCB in the given image is given as

$$\begin{bmatrix}x_{GP}\\ y_{GP}\end{bmatrix}=\sqrt{\frac{S_G}{S_B}}\begin{bmatrix}\cos\theta & -\sin\theta\\ \sin\theta & \cos\theta\end{bmatrix}\begin{bmatrix}x_{BP}-x_{BC}\\ y_{BP}-y_{BC}\end{bmatrix}+\begin{bmatrix}x_{GC}\\ y_{GC}\end{bmatrix} \tag{25}$$

Substituting formula (25) into formula (4), the LOS unit vector can be generated.

5 Experiments

Taking Amathea an irregular celestial body as an example, several experiments are presented to demonstrate the effectiveness and advantages of the proposed system. The 3D model of Amalthea saved in a STL file is a triangular mesh model, as Fig.6 shown. The triangular mesh model contains 20160 facets. The experiments are implemented by MATLAB on a PC with 3.1 GHz, 2GB RAM. Two methods, i.e. the proposed method and a conventional method the FC method, are adopted in the experiments.

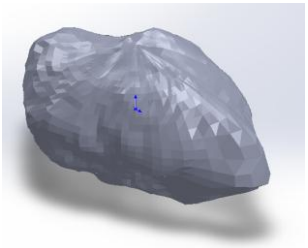

Fig. 6: 3D model of Amalthea

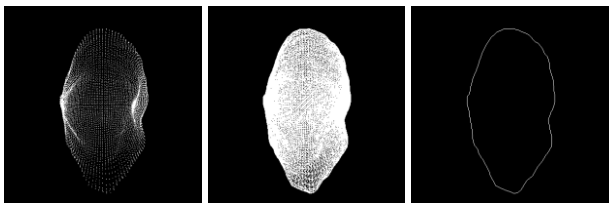

(a)Projected vertexes (b)Projected edges (c) Figure contour

Fig. 7: The process of a figure extraction

For the proposed method, a 2D figure feature database is construed using the 3D model firstly. The sampling interval is set as 3°. Therefore, there are 6962 figures reserved in the database. The time consumption of the database construction is 118 m. Fig. 7 shows the process of a figure extraction from a sampled viewpoint. Fig. 7(a) is the imaging points of all vertexes in the 3D model. Fig. 8(b) is the projected edges of

the 3D model. Fig. 7(c) is the contour of the projected figure. Based on these figures, the chosen features are extracted to construct the 2D figure feature database. Then, a LOS determination system is developed based on the database.

Taking a simulated image of Amalthea as an example, this experiment exhibits the function of the LOS determination system. The size of the image is (512, 512), and the coordinate of the imaging point of CTCB is (256, 256). The image is as Fig. 8(a) shown. Though image processing, the figure contour of the target celestial body is extracted as Fig. 8(b) shown. The proposed method searches out the best matching template of this figure as Fig. 8(c) shown. Finally, the imaging point of CTCB is generated by the proposed method based on the best matching template. Table 1 shows the experiment results. The experiment results demonstrate that the proposed method can achieve high efficiency for LOS detection applied to an irregular celestial body.

Table 1: Experiment results of LOS determination

Parameter	Value
Image size (pixel)	(512, 512)
Real value of imaging point of CTCB (pixel)	(256, 256)
Generated value of imaging point of CTCB (pixel)	(255.5, 256.5)
Error (pixel)	(-0.5, 0.5)
Time consumption (ms)	121

(a) Simulated image (b) Contour of the target (c) Matched template

Fig. 8 The process of LOS determination:

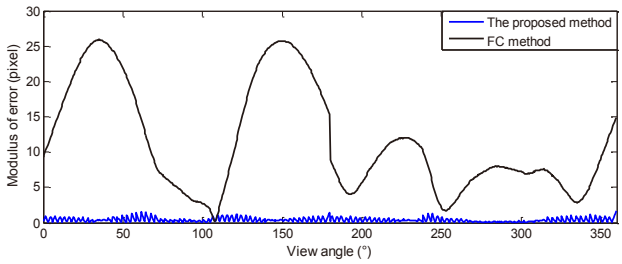

Fig. 9: The results of comparison experiments

Some comparison experiments between the proposed method and the FC method are also introduced. The two methods are both utilized to extract the imaging point of CTCB in some simulated images. A group of simulated images, which are taken around the equator of the target celestial body at regular angle interval of 0.5°, are test through the two methods. The modulus of detection errors are shown in Fig. 9. The experiment results also demonstrate that the proposed method has higher precision than the FC method.

6 Conclusions

This paper proposed a model-based LOS detection system for an irregular target celestial body applied in autonomous optical navigation. The proposed method can achieve high precision for an irregular target body compared with conventional methods. Since the complex geometry of the target celestial body is simplified in the conventional methods, it is difficult for them to achieve high precision solution applied to an irregular target body. On the contrary, the proposed method utilizes the 3D model of the target body to construct a 2D figure feature database. The database reserves the 2D geometry features of the target body. Then, a LOS determination system is developed based on the database. The experimental results demonstrate the proposed method can achieve higher precision compared with a conventional method.

References

[1] H. X. Baoyin, and J. F. Li, A survey on orbital dynamics and navigation of asteroid missions, *Acta Mechanica Sinica*, 30(3): 282-293, 2014.

[2] S. Li, and P. Cui, Landmark tracking based autonomous navigation schemes for landing spacecraft on asteroids, *Acta Astronautica,* 62(6-7) : 391-403, 2008.

[3] X. Ma, J, Fang, and X. Ning, An overview of the autonomous navigation for gravity-assist interplanetary spacecraft, *Progress in Aerospace Sciences* 63: 56-66, 2013.

[4] N. Mastrodemos, D. G. Kubitschek, and S. P. Synnott, Autonomous navigation for the deep impact mission encounter with comet Tempel 1, *Space Science Reviews* 117: 95-121, 2005.

[5] S. Bhaskaran, J. E. Riedel, and S. P. Synnott. Autonomous nucleus tracking for comet/asteroid encounters: the Stardust example, in *Proceedings of Aerospace Conference* 1998: 353-365.

[6] J. A. Christian, and E. G. Lightsey, An on-board image processing algorithm for spacecraft optical navigation sensor system, in *Proceedings of AIAA SPACE 2010 Conference & Exposition*, 2000: 8920.

[7] S. Li, R. Lu, L. Zhang, et al. Image processing algorithms for deep-space autonomous optical navigation, *Journal of navigation* 66(4) : 605-623, 2013.

[8] S. Q. Wu, H. B. Long, and W. H. Zhang, Image processing algorithm for autonomous optical navigation sensor system, *Aerospace Shanghai*, 30(5) : 30-33, 2013.

[9] A. E. Johnson, Y. Cheng, and L. H. Matthies, Machine vision for autonomous small body navigation, in *Proceedings of IEEE Aerospace Conference*, 2000: 661-671.

[10] J. L. Li, and D. W. Zhang, Camera calibration with a near-parallel imaging system based on geometric moments, *Opt. Eng.* 50(2) : 023601, 2011.

[11] M. Li, L. C. Zhang, J. H. M, and et al., Tool-Path Generation for Sheet Metal Incremental Forming Based on STL Model with Defects, *Int. J. Adv . Manuf. Technol.* 63(5-8) : 535-547, 2012.

[12] J. B. Li, and M. Li, Rapid three-dimensional surface mesh segmentation based on region dilation, *Opt. Eng.* 51(5) : 050502, 2012.

[13] Y. Li, Hand gesture recognition using kinect, in *Proceedings of IEEE 3rd International Conference on Software Engineering and Service Science*, 2012: 196-199.

[14] D. Zunic, and J. Zunic, Shape ellipticity based on the first Hu moment invariant, *Information Processing Letters* 113(19-21) : 807-810, 2013.

[15] J. Liu, and T. Zhang, A fast moment algorithm based on link points around shape, *J. Huazhong Univ. of Sci. & Tech. (Nature Science Edition)* 31(1) : 67-69, 2003.